Solar RRL

WILEY VCH

Solar RRL

RESEARCH ARTICLE

Round-Robin Interlaboratory Comparison of Large-Area Organic Thin-Film and Perovskite Solar Cells

Chia-Yuan Chen[1,2] | Yu-Fan Chang[3] | Yen-Chen Shih[3] | Ying-Chuan Liu[2] | Chi-Feng Chiu[2] | Rahma Rahayu Dinarlita[2] | Tsung-Yu Tsai[2] | Chieh-Ming Hung[4] | Hou-Chin Cha[5] | You-Ren Chen[5] | Zhi-Hao Huang[5] | Yu-Cheng Zhang[6] | Hui-Chieh Lin[6] | Wei-Chen Chu[7] | Wei-Hao Chiu[8] | Sie-Rong Li[9] | Ting-Jui Chang[10] | Yi-Hong Liao[10] | Siti Utari Rahayu[11,12] | Bo-Yu Han[13] | Yun-Tou Lin[14] | Pei-Ling Wang[14] | Zi-Ting Liao[14] | Jhao-Yun Tsai[14] | Zhong-En Shi[5] | Chia-Tse Hsu[15] | Po-Shun Hsu[16] | Po-Yuan Chen[17] | Jia-Zhen Li[17] | Anjali Thakran[18,19] | Yu-Ting Chen[20] | Yu-Sheng Li[20] | Hao-Wei Yu[21] | Chu-Chen Chueh[21] | Tzung-Fang Guo[20] | Chih-Wei Chu[18] | Leeyih Wang[17] | Kuo-Chuan Ho[16] | Fang-Chung Chen[15] | Chih-Ping Chen[5] | Yian Tai[14] | Chun-Ting Li[13] | Ming-Way Lee[11] | Chih-Liang Wang[10] | Shih-Sheng Sun[9] | Kun-Mu Lee[7,8,22] | Zong-Liang Tseng[6] | Yu-Ching Huang[5,6,7] | Pi-Tai Chou[4] | Chung-Wen Ko[3] | Chun-Guey Wu[1,2]

[1]Photovoltaic Efficiency Verification Laboratory (PVEVL), National Central University, Taiwan | [2]Department of Chemistry, National Central University, Taiwan | [3]Ways Technical Corp. Ltd., Taoyuan, Taiwan | [4]Department of Chemistry, Center for Emerging Materials and Advanced Devices, National Taiwan University, Taipei, Taiwan | [5]Department of Materials Engineering, Ming Chi University of Technology, New Taipei City, Taiwan | [6]Organic Electronics Research Center, Ming Chi University of Technology, New Taipei City, Taiwan | [7]Department of Chemical and Materials Engineering, College of Engineering, Chang Gung University, Taoyuan, Taiwan | [8]Center for Sustainability and Energy Technologies, Chang Gung University, Taoyuan, Taiwan | [9]Institute of Chemistry, Academia Sinica, Taipei, Taiwan | [10]Department of Materials Science and Engineering, National Tsing Hua University, Hsinchu, Taiwan | [11]Department of Physics and Institute of Nanoscience, National Chung Hsing University, Taichung, Taiwan | [12]Department of Physics, Faculty of Mathematics and Natural Sciences, Universitas Sumatera Utara, Medan, Indonesia | [13]Department of Chemistry, National Taiwan Normal University, Taipei, Taiwan | [14]Department of Chemical Engineering, National Taiwan University of Science and Technology, Taipei, Taiwan | [15]Institute of Electro-Optical Engineering, National Yang Ming Chiao Tung University, Hsinchu, Taiwan | [16]Department of Chemical Engineering, Institute of Polymer Science and Engineering and Advanced Research Center for Green Materials Science and Technology, National Taiwan University, Taipei, Taiwan | [17]Center for Condensed Matter Sciences, National Taiwan University, Taipei, Taiwan | [18]Research Center for Applied Sciences, Academia Sinica, Taipei, Taiwan | [19]Department of Physics, National Taiwan University, Taipei, Taiwan | [20]Department of Photonics and Program on Key Materials, Academy of Innovative Semiconductor and Sustainable Manufacturing, National Cheng Kung University, Tainan, Taiwan | [21]Department of Chemical Engineering, National Taiwan University, Taipei, Taiwan | [22]College of Environment and Resources, Ming Chi University of Technology, Taoyuan, Taiwan

Correspondence: Chia-Yuan Chen (chiayuan@ncu.edu.tw) | Chu-Chen Chueh (cchueh@ntu.edu.tw) | Tzung-Fang Guo (guotf@mail.ncku.edu.tw) | Chih-Wei Chu (gchu@gate.sinica.edu.tw) | Leeyih Wang (leewang@ntu.edu.tw) | Kuo-Chuan Ho (kcho@ntu.edu.tw) | Fang-Chung Chen (fcchendop@nycu.edu.tw) | Chih-Ping Chen (cpchen@mail.mcut.edu.tw) | Yian Tai (ytai@mail.ntust.edu.tw) | Chun-Ting Li (ctli@gapps.ntnu.edu.tw) | Ming-Way Lee (mwl@phys.nchu.edu.tw) | Chih-Liang Wang (wangcl@mx.nthu.edu.tw) | Shih-Sheng Sun (sssun@chem.sinica.edu.tw) | Kun-Mu Lee (KMLee@mail.cgu.edu.tw) | Zong-Liang Tseng (zltseng@mail.mcut.edu.tw) | Yu-Ching Huang (huangyc@mail.mcut.edu.tw) | Pi-Tai Chou (chop@ntu.edu.tw) | Chung-Wen Ko (cw.ko@ways.com.tw) | Chun-Guey Wu (t610002@cc.ncu.edu.tw)

Received: 11 July 2025 | **Revised:** 21 September 2025 | **Accepted:** 28 September 2025

Funding: Advanced Laboratory of Accommodation and Research for Organic Photovoltaics; National Science and Technology Council (NSTC), Taiwan, Grant/Award Numbers: 112-2113-M-008−006 113-2740-M-002−010; Academia Sinica, Grant/Award Number: SV-114-1--18

Keywords: organic thin-film photovoltaics (OPV) | perovskite solar cells (PSC) | round-robin intercomparison | spectral mismatch factor (SMM) | standard test conditions (STC)

ABSTRACT

Organic-thin film and perovskite solar cells are extremely promising because of their rapid progress in photovoltaic conversion efficiency (PCE). Beyond developing new materials and fabrication techniques, accurate performance characterization is essential for research and application. This study reports a round-robin interlaboratory comparison of current density–voltage (J–V) characteristics under standard test conditions (STC) and external quantum efficiency (EQE) spectra for large-area (>1 cm^2) organic

thin-film, perovskite, as well as reference solar cells with distinct spectral responses. Among 20 participating laboratories, the relative deviation in PCE of the samples reaches an unprecedented 111%. A comprehensive analysis identifies critical obstacles to measurement accuracy, including total incident irradiance for the samples, EQE spectrum measurements for spectral mismatch factors (SMM), temperature control, and methodologies for obtaining the *J*–*V* curves. Based on these findings, corresponding recommendations are presented to enhance the accuracy of performance characterization for emerging solar cells.

1 | Introduction

Solar cells' photovoltaic (PV) parameters, particularly the photovoltaic conversion efficiency (PCE), are critical in academic research, commercial production, product applications, and market promotion. For commercial PV technologies, such as monocrystalline silicon, copper indium gallium diselenide (CIGS), and cadmium telluride (CdTe) solar cells and their modules, as well as grid-connected systems, several internationally recognized performance evaluation standards (e.g., IEC 60904 series, IEC 61215, and IEC 61853) [1–3] have been well-established. However, these standards and measurement protocols may not be precisely followed to meet the specific needs of emerging solar cell technologies, such as perovskite solar cells (PSCs), [4, 5] organic thin-film photovoltaics (OPVs), [6, 7] and dye-sensitized solar cells (DSCs), [8, 9] in virtue of their new materials, diverse architectures, and unique characteristics. Although several studies have provided explicit suggestions for performance characterization methods tailored to these new technologies, [10–21] inconsistencies persist in measurement results across laboratories. These inconsistencies should be attributed to variations in equipment specifications, measurement procedures, and personnel training. That poses a significant challenge to achieving international comparability of results and severely hinders the development of emerging solar cell technologies [22].

The best approach to confirm the accuracy of PV parameters is to have internationally accredited standard laboratories directly verify device performance. However, this way has notable limitations, such as restricted access to testing time at authoritative laboratories and the logistical and financial constraints that sample manufacturers might face. Consequently, verified samples are often limited to those with exceptional performance (usually exceeding present PCE records) and adequate environmental stability. To comprehensively and efficiently assess the current status of many laboratories, facilitate collaboration, and improve the accuracy and consistency of PV parameter measurements, a more practical alternative is the implementation of round-robin interlaboratory comparisons [23–43]. This approach enables an efficient and systematic evaluation of measurement capabilities among multiple laboratories to promote international consistency and support the advancement of solar cell technologies.

In this round-robin interlaboratory study organized by the Photovoltaic Efficiency Verification Laboratory (PVEVL) of National Central University (NCU), Taiwan, accredited since 2017 based on ISO/IEC 17025, more than 50 participants from 20 laboratories were involved. Four large-area organic thin-film (OPV-1 and OPV-2) and PSCs (PSC-1 and PSC-2) fabricated according to the literature [44, 45] were used as the samples for the measurements of current density–voltage (*J*–*V*) curves under standard test conditions (STC; AM 1.5 global, 100 mW cm^{-2}, 25°C) [1] and external quantum efficiency (EQE) spectra. Moreover, the data of the commercial crystalline silicon with an optical filter (c-Si + KG) and gallium arsenide (GaAs) reference solar cells (RCs) were also compared to validate the results and identify potential reasons for discrepancies among the laboratories. The photographs (top and side views) and detailed dimensions of the samples are summarized in Figure 1. The OPV and PSC samples (Figure 1a) mounted on black anodized aluminum sheets have identical dimensions

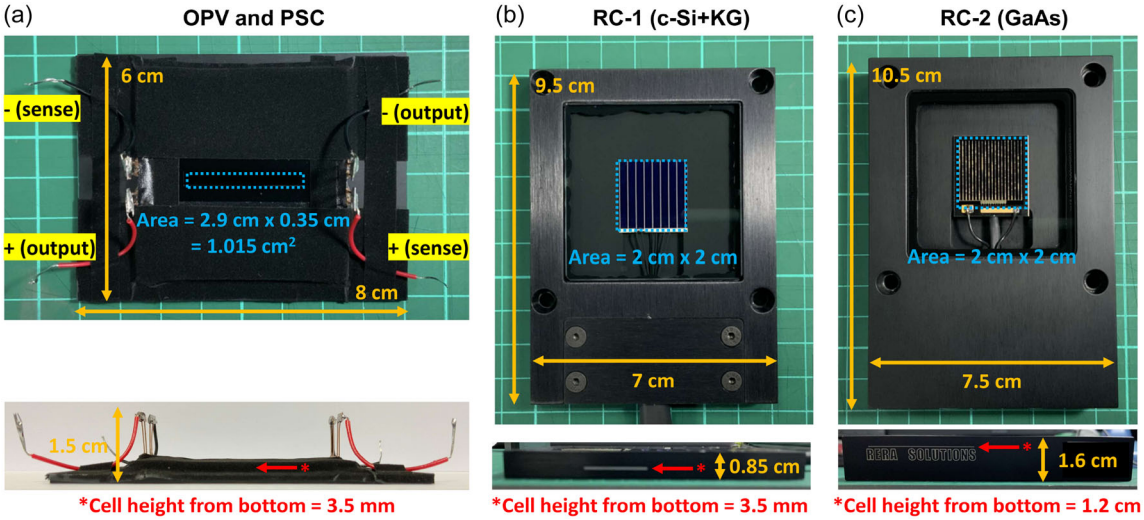

FIGURE 1 | Photographs and detailed dimensions of (a) OPV and PSC, (b) RC-1, and (c) RC-2 samples for round-robin interlaboratory measurements.

for convenient sample alignment. The four-wire (4W) configuration terminals (output and sense) are fixed and labeled to improve the consistency in the comparative results [35, 36, 46, 47]. The area of the samples confined using an aperture of a black and low-reflective metal mask to reduce undesired light reflection and diffusion [35] is 1.015 cm^2, significantly larger than other samples commonly fabricated and characterized by academic research groups. On the other hand, the area of the two RCs is 4 cm^2. The different sample areas (OPVs and PSCs vs. RCs) could help assess the potential discrepancy of the *J–V* measurement caused by the nonuniformity of irradiance. All the participants measured the identical samples and used the same area to calculate the short-circuit current density (J_{sc}) and PCE. The cables for connecting the RCs with a source measurement unit and a temperature sensor (Pt-RTD) are provided with the samples.

2 | Results and Discussion

The *J–V* curves of the six samples measured by the 20 laboratories (the PVEVL and Lab-A ∼ Lab S) under the STC are shown in Figure S1. In this round-robin interlaboratory study, the PVEVL tracked the evolution of PV parameters for all the samples (particularly the OPVs and PSCs) to mitigate the discrepancy arising from the aging of the samples. Therefore, the reliability of comparative results can be confirmed. The initial, midterm, and final PV parameters, as well as the expanded measurement uncertainty (coverage factor (*k*) of 2 for an approximate 95% confidence level) obtained by PVEVL, are summarized in Table S1. As presented in Figure 2, using the initial measurement data of the PVEVL as the reference baseline, the interlaboratory comparison of PCE for the samples reveals a maximum relative deviation of up to 111%. This deviation is calculated as the relative difference between the lowest and highest values (−82% from Lab-F and +29% from Lab-I). Surprisingly, the maximum deviation not only surpasses the other interlaboratory comparisons for emerging PVs [25, 27, 28, 30, 32, 33, 35, 37, 41, 43] but also approaches another round-robin test (maximum deviation of 152%) for indoor low-intensity lighting conditions (using a compact T5 fluorescent light with an illuminance of 600 lx and a color temperature of 6500 K as the light source) [36]. Notably, there is a

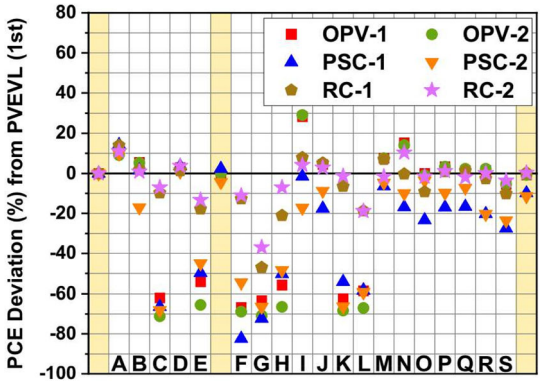

FIGURE 2 | Relative deviation in PCE of the six samples between 20 laboratories. The data from the PVEVL were highlighted in light orange columns to track the stability of the samples. In contrast, other data labeled with letters (A ∼ S) correspond to data measured by different laboratories.

widespread underestimation of PCE across the laboratories. Among the participants, seven laboratories (Lab-C, E, F, G, H, K, and L) report considerably underestimated data (relative deviation >30%), while three laboratories (Lab-A, I, and N) report significant overestimations (relative deviation >10% for some of the samples). For the organic thin-film (OPV-1 and OPV-2) and PSCs (PSC-1 and PSC-2), the misestimations are more pronounced when compared with the reference cells (RC-1 and RC-2). These results highlight the challenges of accurately characterizing the performance of large-area emerging solar cells. Moreover, it is noted that the results of the six samples measured by Lab-A exhibit a systematic drift. In contrast, the deviation among the others for all the samples is diverse. This implies that misleading research directions and strategies may occur even if the researchers focus merely on the "relative comparisons of new solar cells" to explore the potential of new materials or fabrication conditions. In other words, the accuracy of PV parameters is crucial not only to new PCE milestones but also to the demonstrations of new materials and optimization procedures.

A detailed comparison of the PCE, J_{sc}, open-circuit voltage (V_{oc}), and fill factor (FF) for the OPV and PSC samples (Figure 3) also exhibits significant deviations. To mitigate the discrepancy arising from the aging of the OPV and PSC samples, the fitting lines of the PV parameters measured by the PVEVL were included. As presented in Figure 3a, the OPV samples show the maximum PCE deviation reaching 100% (the relative differences range from −71% to +29%), while the maximum deviation of the PSC samples is 96% (the relative differences range from −82% to +14%). It is noted that the extent of PCE deviation significantly surpasses the instability of the samples confirmed by the PVEVL (Table S1; relatively less than −0.8% and −11.5% for the OPVs and PSCs, respectively). In other words, the difference caused by the aging of the samples is negligible. In some laboratories (e.g., Lab-A, I, M, and N), the PCE data are overestimated primarily due to the significantly higher J_{sc} (Figure 3b). Conversely, most of the laboratories reported underestimated V_{oc} (Figure 3c). It is also noted that the deviations in FF (Figure 3d) are generally much more significant than those in J_{sc} and V_{oc}, where severe underestimations are observed from the data of several laboratories (Lab-C, E, F, G, H, K, and L). Similarly, as shown in Figure 3e, the comparative PCE of the reference cells (RC-1 and RC-2) exhibits a maximum deviation of 61% (ranging from −47% (Lab-G) to +14% (Lab-A)). The deviations in other PV parameters (Figure 3f–h) are comparable with those of the OPV and PSC samples.

The correlations between PCE deviation and other PV parameters (J_{sc}, V_{oc}, and FF) are analyzed to diagnose the root causes (Figure 4) quantitatively. The coefficients of determination (R^2) between PCE and the other parameters are 50.9% (J_{sc}), 17.2% (V_{oc}), and 88.0% (FF) for all the samples. These results indicate that the discrepancy in PCE is dominated by FF, followed by J_{sc} and then V_{oc}. The underlying systematic factors for each PV parameter are discussed in the following to investigate the potential causes. Additionally, the corresponding recommendations to improve the accuracy of performance characterization are presented.

(1) Potential reasons affecting the accuracy of J_{sc}: Since all participants used identical sample areas (OPV and PSC = 1.015 cm^2; RC-1 (c-Si + KG) and RC-2 (GaAs) = 4 cm^2 in Figure 1),

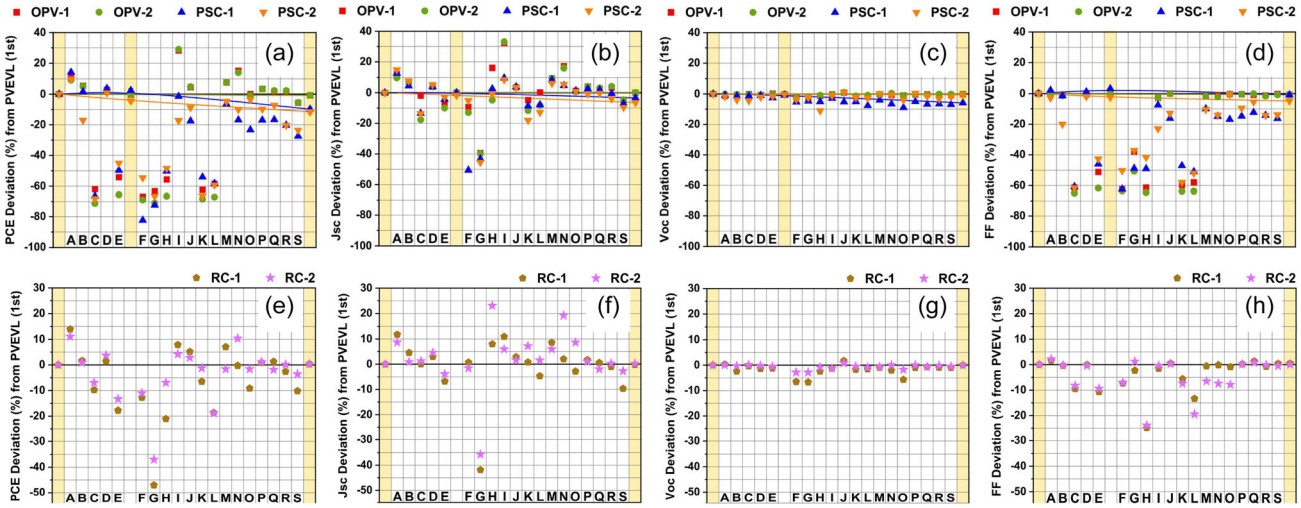

FIGURE 3 | Relative deviations in (a,e) PCE, (b,f) J_{sc}, (c,g) V_{oc}, and (d,h) FF of OPV, PSC, and RC samples between 20 laboratories. The data from the PVEVL were highlighted in light orange columns, while other data labeled with letters (A ~ S) correspond to data measured by different laboratories. In (a–d), the fitting lines are based on the PVEVL's data to mitigate the discrepancy arising from the aging of the OPV and PSC samples.

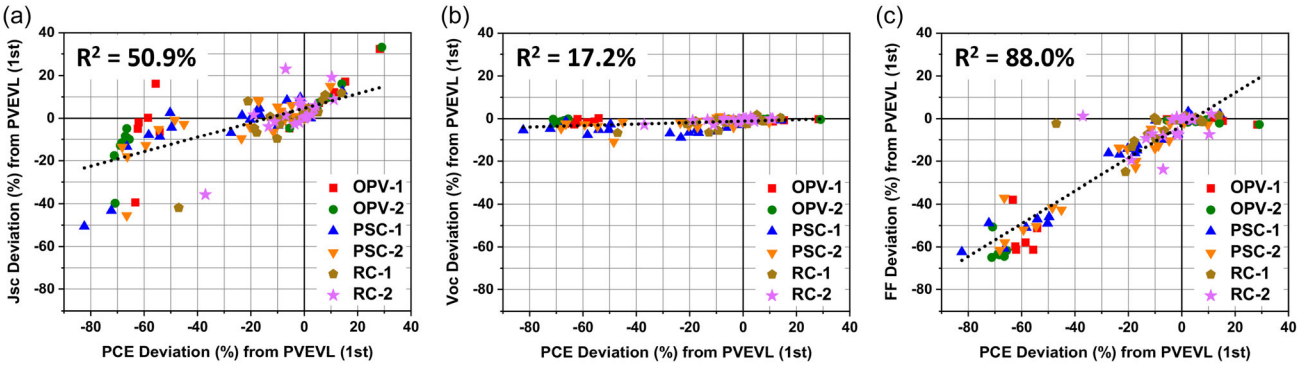

FIGURE 4 | Correlation diagrams of PCE deviations between (a) J_{sc}, (b) V_{oc}, and (c) FF of the samples measured by 20 laboratories.

variations in J_{sc} should be mainly related to the following factors: (a) Solar simulator performance: The specifications of the solar simulator directly affect the accuracy of J_{sc} measurements. Among the criteria of spectral match, nonuniformity of irradiance in the test plane, and temporal instability of irradiance filed in IEC 60904–9 [48] for classifying solar simulator characteristics, the nonuniformity should be noted particularly. This is due to the designated area of OPV and PSC samples (2.9 cm × 0.35 cm) being distinct from that of typical RCs (2.0 cm × 2.0 cm). In addition to the periodic measurement of the nonuniformity, it is recommended that the averaged irradiance obtained from multiple pixels matching the areas of samples and RCs should be used to eliminate the difference in irradiance between them. After all, the areas of emerging PV samples for academic research (usually less than 1 cm^2) might differ from those of RCs (typically 4 cm^2). (b) Lack of suitable RCs: Unlike widely commercialized PV products, the OPV and PSC samples used in this study do not have standardized RCs showing precisely the same EQE spectra. (c) Reference solar cell calibration: Differences in the type, usage, maintenance, and calibration accuracy of RCs used for adjusting and verifying the total irradiance of solar simulator output play a significant role in the *J–V* curves measurements of PV samples. As displayed in Figure S2a,b, the correlation of J_{sc} deviation between the emerging PVs and the two RC samples implies that in the EQE spectra of RCs, the participants used to adjust the total irradiance of their solar simulators should be closer to RC-1 (c-Si + KG) because of the coefficient of determination ($R^2 = 60.3\%$) higher than RC-2 (GaAs; $R^2 = 46.4\%$). However, the low R^2 suggests that the measurement procedures of some of the participants should be adjusted, in addition to the recalibration of the RCs to validate the accuracy and traceability of measurement results.

It is a fact that no solar simulator can precisely replicate the AM 1.5G standard spectrum [49]. Thus, the spectral mismatch factor (SMM) filed in IEC 60904–7 [50] is essential for enhancing the accuracy of J_{sc} and other PV parameters. Furthermore, it is crucial to emphasize that the J_{sc} corrected using the SMM is more reliable than the cross-check with the value calculated from the overlap integral [51] of the EQE spectrum with the AM 1.5G standard spectrum. The normalized EQE spectra of all samples are thus compared to evaluate the participants' capabilities for the SMM. As displayed in Figure S3, five laboratories (Lab-F, H, L, M, and S) could not provide EQE spectral data for comparison, implying their inability to verify the accuracy of PV data independently. Additionally, severe deviations are observed in the spectral data from a few laboratories (e.g., Lab-E, G, and N), while minor differences are present in the others. Due to the various

wavelength intervals applied across the laboratories (ranging from 1 to 50 nm), the centroid wavelength (λ_c) of all normalized EQE spectra was calculated using Equation (1) [35] as a quantitative method to evaluate the differences. The centroid wavelength (λ_c), compared with the maximum wavelength (λ_{max}) and onset wavelength (λ_{onset}) commonly applied in academic research, renders a more comprehensive representation of waveform differences in EQE spectra. This approach is a reliable metric for assessing whether laboratories can accurately determine the SMM, ultimately increasing the precision of PV parameter measurements, particularly J_{sc}.

$$\lambda_c = \frac{\int \mathrm{EQE}(\lambda) \times \lambda d\lambda}{\int \mathrm{EQE}(\lambda)\, d\lambda} \quad (1)$$

It is worth mentioning that the PVEVL can measure EQE spectra of all PV samples using diverse measurement configurations, including direct current (DC), alternating current (AC), and alternating current with white-biased light (AC + WB) modes [35]. This capability helps identify unique characteristics of emerging PV samples (such as nonlinearity and slow response) that differ from the behaviors of single-crystalline silicon solar cells. As presented in Figure 5, both OPV-1 and PSC-1, measured using different measurement methods, exhibit variations in their normalized EQE spectra, confirming their nonlinearity. These data suggest that applying white-biased light (the AC + WB mode) in the measurements is crucial to ensure that the EQE spectra can precisely represent the faithful performance of the nonlinear responsive samples under the STC. That means the EQE spectra of nonlinearly responsive samples should be measured under the desired operation level (similar or identical to the AM 1.5G). If the white-biased light is not applicable due to the limitation of equipment, varying the intensity of monochromatic light using neutral density filters is recommended as an alternative way to evaluate the nonlinearity of the samples. As a result, the improved precision of SMM can contribute to the accuracy of *J*–*V* curves and the corresponding PV parameters. As summarized in Table 1, the nonlinearity of OPV-1 and PSC-1 results in λ_c variations of up to ±0.8 nm for OPV-1 and ±3.1 nm for PSC-1, indicating that deviations within the ranges should be mainly due to different measurement modes. In other words, the scopes can serve as benchmarks for assessing the accuracy and suitability of EQE measurement equipment and parameter settings used by the participants.

TABLE 1 | Centroid wavelengths (λ_c) of normalized EQE spectra for OPV-1 and PSC-1 measured by the PVEVL using various modes.

Sample/ Mode	DC [nm]	AC-97 Hz [nm]	AC-97 Hz with WB [nm]	AC-13 Hz with WB [nm]
OPV-1	610.7	610.4	611.0	611.2
PSC-1	565.6	564.9	568.0	565.8

Figure 6 presents deviations in the λ_c of all normalized EQE spectra for the six samples, using the data of the PVEVL as the reference. Only Lab-D achieves λ_c deviations within ±3.1 nm among the participating laboratories for all the samples. In contrast, significant discrepancies exceeding ±10 nm are observed for the specific samples measured by several laboratories. For example, Lab-E and Lab-I showed substantial deviations in the λ_c of OPV-1, while Lab-E, N, and P have similar issues in OPV-2. Notable deviations in PSC-1 and PSC-2 are observed in Lab-E, O, P, and N. Besides, Lab-E and G reported shifted λ_c in the cases of RC-1 and RC-2. These results reveal the urgent need for many participants to fine-tune and reassess their EQE measurement systems. Careful consideration should be given to light source stability, monochromator dispersion, wavelength shifts, and the calibration of photodiodes (or RCs) used as external light detectors.

(2) Potential reasons affecting the accuracy of V_{oc}: As shown in Figure 7a, a comparison of V_{oc} data for the six samples reveals that most laboratories reported significantly lower values, particularly for PSC-1 and PSC-2. Considering the V_{oc} variation of all the samples, the maximum deviation reaches ≈10% (Lab-H). According to the literature, [46, 52–61] sample temperature significantly impacts V_{oc} measurements. In general, a higher sample temperature will lead to a substantial underestimation of V_{oc}. This explains why the STC includes not only incident light specifications (AM 1.5G) but also a requirement to maintain the sample temperature at 25°C [1]. As shown in Figure 7b, the relative temperature coefficients of V_{oc} measured by the PVEVL for OPV-1, PSC-1, RC-1, and RC-2 are *ca.* −0.12, −0.20, −0.38,

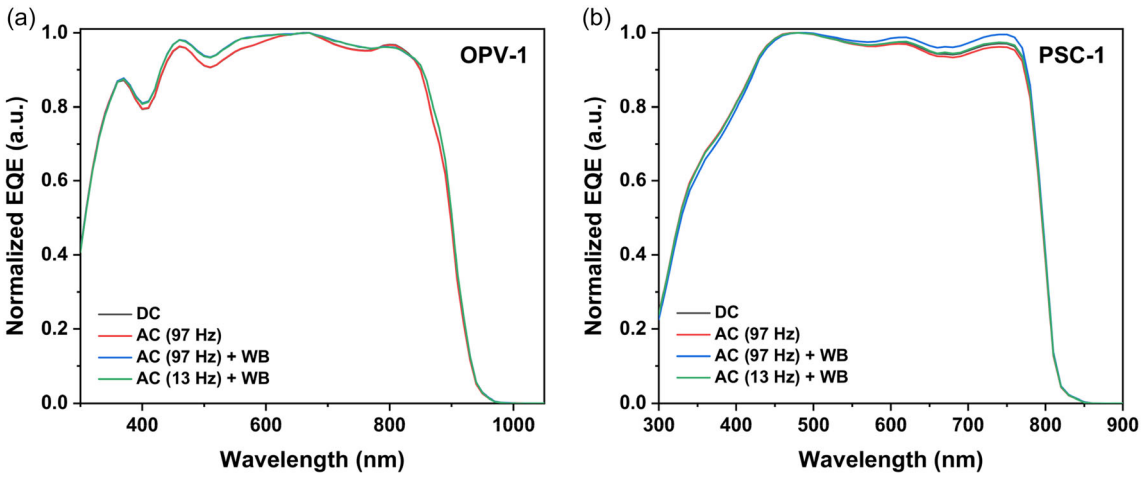

FIGURE 5 | Normalized EQE spectra of (a) OPV-1 and (b) PSC-1 measured by the PVEVL using various modes.

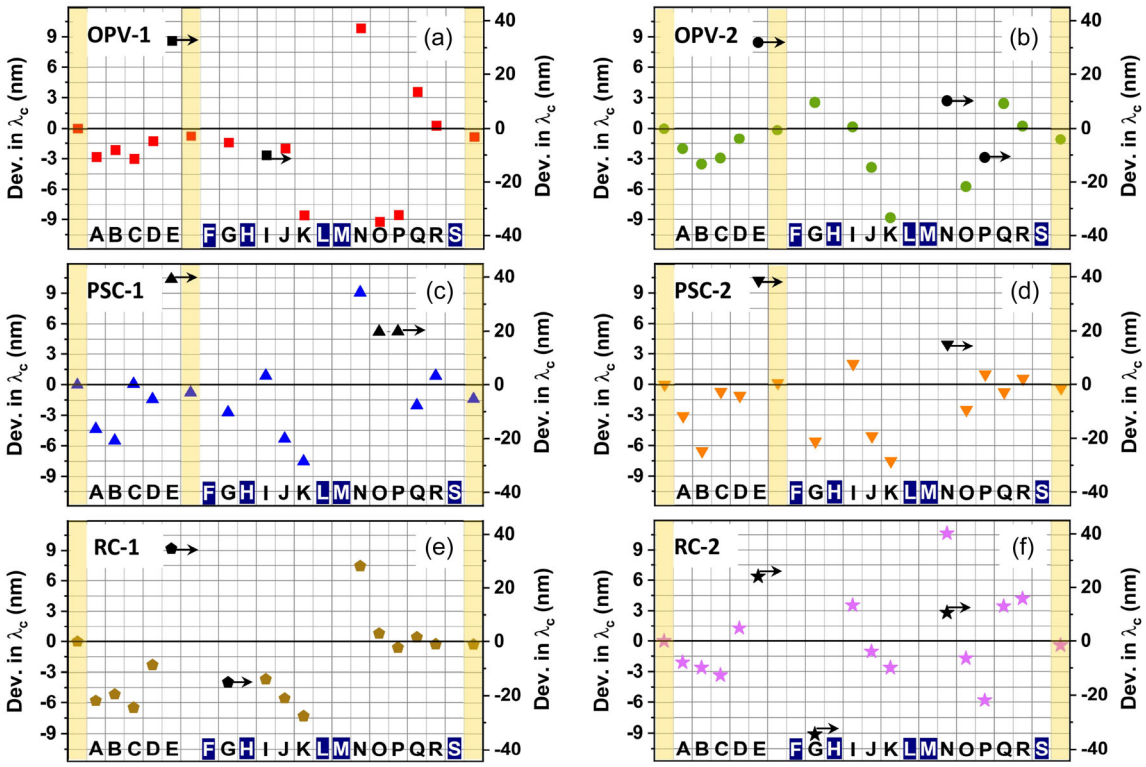

FIGURE 6 | Deviations in centroid wavelength (λ_c) of all normalized EQE spectra for (a) OPV-1, (b) OPV-2, (c) PSC-1, (d) PSC-2, (e) RC-1, and (f) RC-2. The data from the PVEVL were highlighted in light orange columns. The other data labeled with letters (A ~ S) correspond to data measured by different laboratories, in which Lab-F, H, L, M, and S, labeled in white, indicate the unavailability of the EQE spectra for comparison.

and $-0.19\%°C^{-1}$, respectively. On the other hand, the correlation of V_{oc} deviation between the emerging PVs and the two RC samples (Figure S2c,d) shows that the V_{oc} of PSC samples is underestimated to a greater magnitude than that of OPVs. The comparable coefficients of determination ($R^2 = 57.2\%$ and 54.9%) imply that most participants might not precisely control the temperature of the two RC samples through the integrated Pt-RTD temperature sensors. These results suggest that sample temperature should be carefully monitored and controlled for performance characterization, especially for PSC samples in this study exhibiting both activation and hysteresis [16, 17, 57, 59, 60, 62] phenomena in their *J–V* characteristics. This is because continuous illumination is inevitably required in the measurements for such samples to reach a metastable state. Besides, extending the measurement duration (i.e., reducing the scan rate) is a popular strategy to minimize deviations caused by the hysteresis. Without appropriate temperature control, the sample temperature will easily exceed 25°C during continuous exposure to simulated sunlight. The rise in sample temperature would be especially problematic for PSCs, eventually resulting in an underestimated V_{oc}. Precise thermal management of samples using a temperature-programmable stage, a T-type (or K-type) thermocouple or a Pt-RTD temperature sensor, and a periodically calibrated thermal monitor is thus recommended to improve the accuracy of V_{oc}. As demonstrated in Figure S4, the OPV/PSC sample mounted on a black anodized aluminum sheet should be fixed adequately on a temperature-programmable stage. For the temperature monitor and control of the sample, a T-type thermocouple could be used (to contact with the non-conductive aluminum sheet), and a thermal pad should be inserted between the thermocouple and the stage for better thermal conduction. Finally, a light-shielding cover should be placed at the top to eliminate undesired light reflection in *J–V* measurements.

(3) Potential reasons affecting the accuracy of FF: As shown in Figure 7c, Lab-C, E, F, G, H, K, and L reported substantial underestimations of FF for all samples (especially OPVs and PSCs), with relative deviations exceeding 20%. This underestimation is a dominant factor in these laboratories' significantly low PCE values (Figures 2 and 4c). On the other hand, the FF of PSC samples measured by Lab-B, I, J, N, O, P, Q, R, and S show deviations exceeding 10%. According to the Shockley solar cell equations, [63–65] an increase in sample temperature above the standard condition of 25°C not only leads to underestimation of V_{oc} but also tends to produce significantly lower FF values. However, as presented in Figure 7d, the relative temperature coefficients of FF measured by the PVEVL for OPV-1 and PSC-1 are *ca.* 0.09 and $0.32\%°C^{-1}$. In contrast to the coefficients of RC-1 ($-0.10\%°C^{-1}$) and RC-2 ($-0.07\%°C^{-1}$), the positive thermal dependence of OPV-1 and PSC-1 should be attributed to the decrease in interfacial resistance between the heterojunctions and the intrinsic increase in conductivity of the materials under rising temperature [61]. These results indicate that other factors beyond the temperature coefficients result in the underestimated FF for the OPVs and PSCs.

To explore the causes of substantially underestimated FF, the PVEVL conducted additional measurements using OPV-1 and PSC-1 samples to compare the PV parameters obtained via

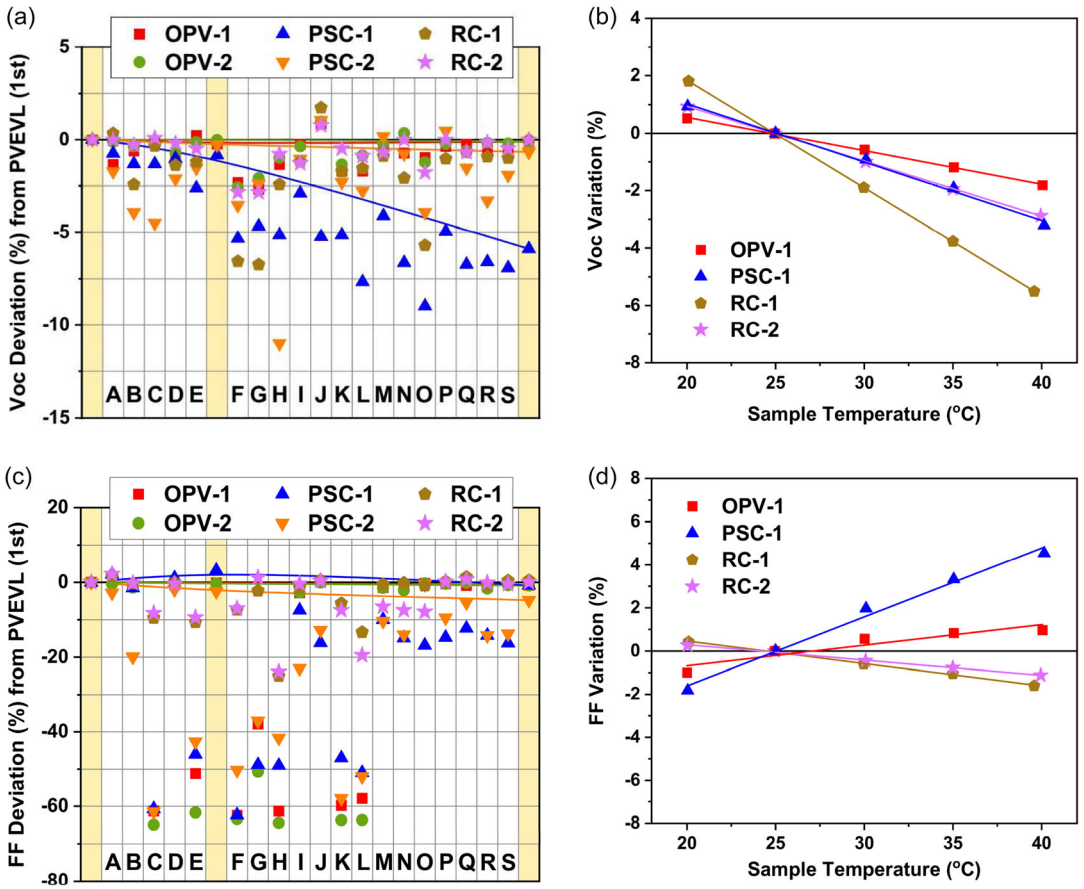

FIGURE 7 | Relative deviations in (a) V_{oc} and (c) FF of six samples between 20 laboratories. The data from the PVEVL were highlighted in light orange columns, while other data labeled with letters (A ~ S) correspond to data measured by different laboratories. The fitting lines for OPVs and PSCs are based on the PVEVL's data. Temperature dependence of (b) V_{oc} and (d) FF for OPV-1, PSC-1, RC-1, and RC-2.

two-wire (2W) and 4W methods. As shown in Figure 8, regardless of sample type, the 2W method consistently produced significant underestimations of FF, along with lower V_{oc} and J_{sc} values. This scenario results from the fact that the 2W measurements are greatly affected by the resistance of connecting wires and parasitic resistance inside the measuring samples and source measurement units. Moreover, these resistances induce voltage drops (IR drops) that become more pronounced in larger-area samples showing high output currents. Based on this and previous reports, [35, 36, 46, 47] the OPV and PSC samples used in this study were equipped with four fixed electrodes for connections, explicitly labeled with polarity (+/−) and output/sense terminals (Figure 1) to improve measurement consistency. However, as summarized in Table 2, the relative deviations in FF for OPV-1 and PSC-1 are up to −59.7% and −40.9%, respectively. These deviations and the shapes of *J*–*V* curves (Figure S1) closely align with the extent of the underestimated FF reported by Lab-C, E, F, G, H, K, and L. Furthermore, the correlation of FF deviation between the emerging PVs and the two RC samples (Figure S2e,f) shows that the FF of OPV samples is more underestimated than that of PSCs, which should be due to the current of the former samples being higher than that of the latter cases (Figure 8). Compared with the coefficient of determination based on RC-2 ($R^2 = 42.5\%$), the larger coefficient for RC-1 ($R^2 = 59.0\%$) should be attributed to the fact that the FF is closer to those of the OPVs and PSCs (Table S1). These results indicate that the severe

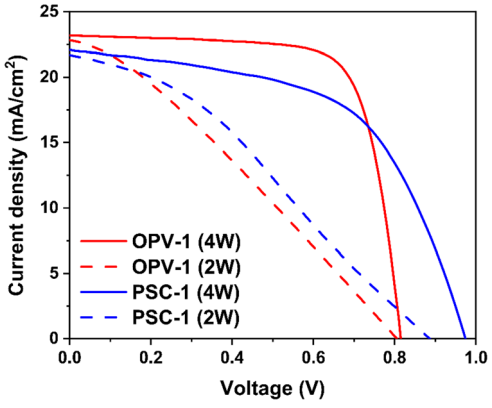

FIGURE 8 | *J*–*V* curves of OPV-1 and PSC-1 measured using two-wire (2W) and four-wire (4W) methods.

TABLE 2 | Relative deviation in PV parameters of OPV-1 and PSC-1 measured with different methods (2W vs. 4W).

Sample[a]	J_{sc} [%]	V_{oc} [%]	FF [%]	PCE [%]
OPV-1	−1.5	−1.1	−59.7	−60.8
PSC-1	−1.8	−9.1	−40.9	−47.3

[a]The relative deviations are calculated using PV parameters from the 4W method as the standard.

FF underestimations reported by the participants should be caused by limitations in measurement equipment (e.g., using only a potentiostat to measure *J–V* curves) or inadequate personnel training (e.g., failure to set the measurement mode), resulting in reliance on the 2W method. To address this issue, proper source measurement units and the 4W configuration must be applied in the measurement, particularly for large-area PV samples showing high output currents.

As aforementioned, it is found that the PSC samples used in this study exhibited both hysteresis and activation phenomena. To eliminate the hysteresis and ensure the accuracy of PV parameters for PSC samples, the following four techniques have been proposed [21]: (1) conventional *J–V* measurement using continuous voltage sweep with longer sampling delay time (Td), (2) acquisition of stabilized current at a fixed voltage approaching maximum power point voltage (Vmax), (3) maximum power point tracking (MPPT) for stabilized output power, and (4) dynamic *J–V* technique to held samples at specific voltages for a long while. A comparison of the advantages and disadvantages of these techniques is summarized in Table 3.

In this study, most participants used the technique (1) for convenience. However, as illustrated in Figure 9a (using PSC-1 as an example), insufficient Td (e.g., 10 ms) applied with the forward scan mode (from low voltage near J_{sc} to high voltage near V_{oc}) for the *J–V* curve measurements led to ≈−6% FF deviation and +2% J_{sc} deviation. Therefore, a longer Td (such as 30 s) is strongly recommended to obtain the stabilized and faithful PV parameters. As the data provided by the PVEVL (Figure S1) using the technique (4), the holding voltages could be limited to the points near J_{sc}, maximum output power (Pmax) density, and V_{oc} for saving measurement time. Furthermore, as displayed in Figure 9b, preconditioning of the PSC-1 sample using the continuous

TABLE 3 | Comparison of various *J–V* measurement techniques.

#	Technique	Advantages	Disadvantages
1	Conventional *J–V* measurement	(a) Simple for labs. (b) Longer delay time (Td) could reduce capacitive effects and yield stable values.	(a) Time-consuming for measuring many data points. (b) Might not completely mitigate the hysteresis of PSCs.
2	Stabilized current acquisition at a fixed voltage near V_{max}	(a) Relatively quick to implement. (b) Directly yields a stabilized current to validate the maximum power point.	(a) Lacks a full *J–V* curve for PV parameters. (b) Sensitive to the selected voltage, which might shift during measurement.
3	Maximum power point tracking (MPPT)	(a) Provides steady-state output power and PCE. (b) Considered the most reliable method for device performance characterization.	(a) More sophisticated instrumentation and longer measurement time. (b) The precision highly depends on the algorithm used for tracking.
4	Dynamic *J–V* technique (holding at specific voltages for extended times)	(a) Probes transient and steady-state behaviors at selected voltages. (b) Useful for studies of hysteresis, ion migration, and stability.	(a) Needs careful choices of voltages and hold times. (b) Might accelerate the degradation of samples due to prolonged bias stress.

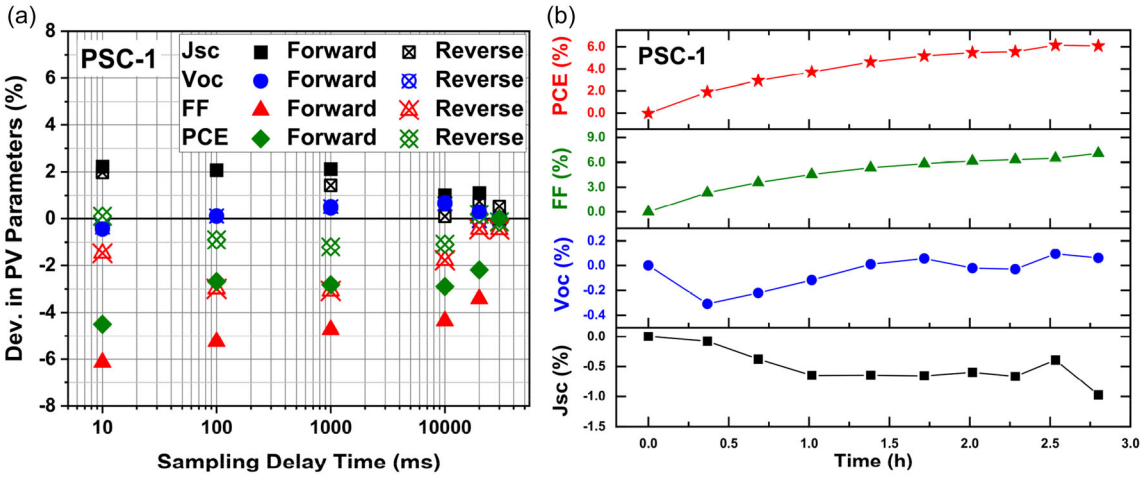

FIGURE 9 | (a) Relative deviations in PV parameters of PSC-1 measured with various sampling delay times and different sweeping directions (forward scanning from low voltage near J_{sc} to high voltage near V_{oc}, and the reverse way). (b) Relative variations in PV parameters of PSC-1 under continuous irradiation of simulated sunlight and sample temperature at 25 ± 1°C.

irradiation of simulated sunlight (light-soaking) for at least 2 h should be required to achieve the metastable state; otherwise, an underestimation of FF by ≈6% and a deviation in J_{sc} of around +1% might be obtained. The increased FF upon the continuous light-soaking might be due to the improved defect passivation or the built-in potential induced by ion migration. [66–69] It is worth highlighting that the optimal preconditioning for various PSCs could be varied and unpredictable because of the diverse materials and nanoscopic features. Therefore, the timely tracking of the evolution of PV parameters (with rapid and successive *J–V* measurements) for each PSC sample under continuous light-soaking should practically be the best practice to alleviate the measurement errors caused by the activation.

3 | Conclusion

This round-robin interlaboratory comparison highlights the critical challenges in accurately characterizing the performance of large-area OPVs and PSCs. The unprecedented 111% relative deviation in PCE measurements among the 20 laboratories suggests the urgent need for standardized characterization protocols and improved accuracy in key measurements. Specifically, (1) EQE spectrum measurements using AC + WB mode and a precisely calibrated external light detector, calculation of SMM, periodic calibration of RCs, and the averaged irradiance from multiple pixels are recommended to improve the accuracy of total incident irradiance and J_{sc} for various PV samples, (2) precise temperature control of samples using a temperature-programmable stage, thin-film T or K-type thermocouple (or a Pt-RTD temperature sensor), and a periodically calibrated thermal monitor is essential to improve the accuracy of V_{oc}, and (3) 4W measurement methods to reduce IR-drops, the extended sampling delay time for obtaining *J–V* curves, and continuous light-soaking of samples combined with timely tracking the evolution of PV parameters under controlled temperature to reach a metastable state are recommended for accurate FF, in particular for PSC samples showing hysteresis and activation. These recommendations proposed for the performance characterization can enhance measurement reliability and reproducibility to fairly rank new materials and techniques for advancing the research and application of emerging PV technologies.

Acknowledgements

The Advanced Laboratory of Accommodation and Research for Organic Photovoltaics (AROPV), the National Science and Technology Council (NSTC), Taiwan, Republic of China, and financial support from the NSTC, Taiwan, Republic of China (Grant no. 112-2113-M-008−006 and 113-2740-M-002−010 (A-Core Plus Project)) and Academia Sinica (Grant no. SV-114-1-18), Taiwan, Republic of China are gratefully acknowledged.

Conflicts of Interest

The authors declare no conflicts of interest.

Data Availability Statement

The data that support the findings of this study are available from the corresponding author upon reasonable request.

References

1. IEC, Photovoltaic Devices – Part 1: Measurement of Photovoltaic Current-Voltage Characteristics, IEC 60904-1:2020, (International Electrotechnical Commission, 2020).

2. IEC, Terrestrial Photovoltaic (PV) Modules - Design Qualification and Type Approval – Part 1: Test Requirements, IEC 61215-1:2021, (International Electrotechnical Commission, 2021).

3. IEC, Photovoltaic (PV) Module Performance Testing and Energy Rating – Part 1: Irradiance and Temperature Performance Measurements and Power Rating, IEC 61853-1:2011, (International Electrotechnical Commission, 2011).

4. J. Y. Kim, J. W. Lee, H. S. Jung, H. Shin, and N. G. Park, "High-Efficiency Perovskite Solar Cells," *Chemical Reviews* 120 (2020): 7867–7918.

5. P. Chen, Y. Xiao, and S. Li, et al., "The Promise and Challenges of Inverted Perovskite Solar Cells," *Chemical Reviews* 124 (2024): 10623–10700.

6. L. Lu, T. Zheng, Q. Wu, A. M. Schneider, D. Zhao, and L. Yu, "Recent Advances in Bulk Heterojunction Polymer Solar Cells," *Chemical Reviews* 115 (2015): 12666–12731.

7. E. K. Solak and E. Irmak, "Advances in Organic Photovoltaic Cells: A Comprehensive Review of Materials, Technologies, and Performance," *RSC Advances* 13 (2023): 12244–12269.

8. A. Hagfeldt, G. Boschloo, L. Sun, L. Kloo, and H. Pettersson, "Dye-Sensitized Solar Cells," *Chemical Reviews* 110 (2010): 6595–6663.

9. B. Pashaei, H. Shahroosvand, M. Grätzel, and M. K. Nazeeruddin, "Influence of Ancillary Ligands in Dye-Sensitized Solar Cells," *Chemical Reviews* 116 (2016): 9485–9564.

10. K. Hara, S. Igari, S. Takano, and G. Fujihashi, "Characterization of Photovoltaic Performance of Dye-Sensitized Solar Cells," *Electrochemistry* 73 (2005): 887–896.

11. V. Shrotriya, G. Li, Y. Yao, T. Moriarty, K. Emery, and Y. Yang, "Accurate Measurement and Characterization of Organic Solar Cells," *Advanced Functional Materials* 16 (2006): 2016–2023.

12. H. J. Snaith, "How Should You Measure Your Excitonic Solar Cells?," *Energy & Environmental Science* 5 (2012): 6513–6520.

13. H. J. Snaith, "The Perils of Solar Cell Efficiency Measurements," *Nature Photonics* 6 (2012): 337–340.

14. X. Yang, M. Yanagida, and L. Han, "Reliable Evaluation of Dye-Sensitized Solar Cells," *Energy & Environmental Science* 6 (2013): 54–66.

15. K. Takagi, S. Magaino, H. Saito, T. Aoki, and D. Aoki, "Measurements and Evaluation of Dye-Sensitized Solar Cell Performance," *Journal of Photochemistry and Photobiology C: Photochemistry Reviews* 14 (2013): 1–12.

16. H. J. Snaith, A. Abate, J. M. Ball, et al., "Anomalous Hysteresis in Perovskite Solar Cells," *Journal of Physical Chemistry Letters* 5 (2014): 1511–1515.

17. E. L. Unger, E. T. Hoke, C. D. Bailie, et al., "Hysteresis and Transient Behavior in Current–Voltage Measurements of Hybrid-Perovskite Absorber Solar Cells," *Energy & Environmental Science* 7 (2014): 3690–3698.

18. J. A. Christians, J. S. Manser, and P. V. Kamat, "Best Practices in Perovskite Solar Cell Efficiency Measurements. Avoiding the Error of Making Bad Cells Look Good," *Journal of Physical Chemistry Letters* 6 (2015): 852–857.

19. Y. Hishikawa, H. Shimura, T. Ueda, A. Sasaki, and Y. Ishii, "Precise Performance Characterization of Perovskite Solar Cells," *Current Applied Physics* 16 (2016): 898–904.

20. E. Zimmermann, K. K. Wong, M. Müller, et al., "Characterization of Perovskite Solar Cells: Towards a Reliable Measurement Protocol," *APL Materials* 4 (2016): 091901.

21. G. Bardizza, H. Müllejans, D. Pavanello, and E. D. Dunlop, "Metastability in Performance Measurements of Perovskite PV Devices: A Systematic Approach," *Journal of Physics: Energy* 3 (2021): 021001.

22. E. Zimmermann, P. Ehrenreich, T. Pfadler, J. A. Dorman, J. Weickert, and L. Schmidt-Mende, "Erroneous Efficiency Reports Harm Organic Solar Cell Research," *Nature Photonics* 8 (2014): 669–672.

23. D. L. King, B. R. Hansen, and J. K. Jackson, "*Sandia/NIST Reference Cell Calibration Procedure*," in Conference Record of the IEEE Photovoltaic Specialists Conference, (IEEE, 1993), 1095–1101.

24. C. R. Osterwald, S. Anevsky, K. Bücher, et al., "The World Photovoltaic Scale: An International Reference Cell Calibration Program," *Progress in Photovoltaics: Research and Applications* 7 (1999): 287–297.

25. F. C. Krebs, S. A. Gevorgyan, B. Gholamkhass, et al., "A Round Robin Study of Flexible Large-Area Roll-to-Roll Processed Polymer Solar Cell Modules," *Solar Energy Materials and Solar Cells* 93 (2009): 1968–1977.

26. M. Pravettoni, R. Galleano, R. Fucci, et al., "Characterization of High-Efficiency c-Si CPV Cells," *Progress in Photovoltaics: Research and Applications* 19 (2011): 898–907.

27. S. A. Gevorgyan, A. J. Medford, E. Bundgaard, et al., "An Inter-Laboratory Stability Study of Roll-to-Roll Coated Flexible Polymer Solar Modules," *Solar Energy Materials and Solar Cells* 95 (2011): 1398–1416.

28. T. T. Larsen-Olsen, F. Machui, B. Lechene, et al., "Round-Robin Studies as a Method for Testing and Validating High-Efficiency ITO-Free Polymer Solar Cells Based on Roll-to-Roll-Coated Highly Conductive and Transparent Flexible Substrates," *Advanced Energy Materials* 2 (2012): 1091–1094.

29. Y. Hishikawa, H. Liu, H. H. Hsieh, et al., "Round-Robin Measurement Intercomparison of c-Si PV Modules Among Asian Testing Laboratories," *Progress in Photovoltaics: Research and Applications* 21 (2013): 1181–1188.

30. T. T. Larsen-Olsen, S. A. Gevorgyan, R. R. Søndergaard, et al., "A Round Robin Study of Polymer Solar Cells and Small Modules Across China," *Solar Energy Materials and Solar Cells* 117 (2013): 382–389.

31. R. Galleano, W. Zaaiman, A. Virtuani, et al., "Intercomparison Campaign of Spectroradiometers for A Correct Estimation of Solar Spectral Irradiance: Results and Potential Impact on Photovoltaic Devices Calibration," *Progress in Photovoltaics: Research and Applications* 22 (2014): 1128–1137.

32. S. A. Gevorgyan, O. Zubillaga, J. M. V. Seoane, et al., "Round Robin Performance Testing of Organic Photovoltaic Devices," *Renewable Energy* 63 (2014): 376–387.

33. M. V. Madsen, S. A. Gevorgyan, R. Pacios, et al., "Worldwide Outdoor Round Robin Study of Organic Photovoltaic Devices and Modules," *Solar Energy Materials and Solar Cells* 130 (2014): 281–290.

34. E. Salis, D. Pavanello, M. Field, et al., "Improvements in World-Wide Intercomparison of PV Module Calibration," *Solar Energy* 155 (2017): 1451–1461.

35. C. Y. Chen, S. K. Ahn, D. Aoki, et al., "International Round-Robin Inter-Comparison of Dye-Sensitized and Crystalline Silicon Solar Cells," *Journal of Power Sources* 340 (2017): 309–318.

36. C. Y. Chen, Z. H. Jian, S. H. Huang, et al., "Performance Characterization of Dye-Sensitized Photovoltaics under Indoor Lighting," *Journal of Physical Chemistry Letters* 8 (2017): 1824–1830.

37. R. B. Dunbar, B. C. Duck, T. Moriarty, et al., "How Reliable Are Efficiency Measurements of Perovskite Solar Cells? The First Inter-Comparison, Between Two Accredited and Eight Non-Accredited Laboratories," *Journal of Materials Chemistry A* 5 (2017): 22542–22558.

38. C. Monokroussos, E. Salis, D. Etienne, et al., "Electrical Characterization Intercomparison of High-Efficiency c-Si Modules Within Asian and European Laboratories," *Progress in Photovoltaics: Research and Applications* 27 (2019): 603–622.

39. E. Salis, D. Pavanello, I. Kröger, et al., "Results of Four European Round-Robins on Short-Circuit Current Temperature Coefficient Measurements of Photovoltaic Devices of Different Size," *Solar Energy* 179 (2019): 424–436.

40. M. Bliss, T. Betts, R. Gottschalg, et al., "Interlaboratory Comparison of Short-Circuit Current versus Irradiance Linearity Measurements of Photovoltaic Devices," *Solar Energy* 182 (2019): 256–263.

41. E. Salis, A. Gerber, J. W. Andreasen, et al., "A European Proficiency Test on Thin-Film Tandem Photovoltaic Devices," *Progress in Photovoltaics: Research and Applications* 28 (2020): 1258–1276.

42. M. R. Vogt, S. Riechelmann, A. M. G. Amillo, et al., "PV Module Energy Rating Standard IEC 61853-3 Intercomparison and Best Practice Guidelines for Implementation and Validation," *IEEE Journal of Photovoltaics* 10 (2022): 844–852.

43. H. Saito, M. Yoshita, H. Tobita, et al., "Round-Robin Inter-Comparison of Maximum Power Measurement for Metastable Perovskite Solar Cells," *ECS Journal of Solid State Science and Technology* 11 (2022): 055008.

44. M. A. Green, E. D. Dunlop, J. Hohl-Ebinger, M. Yoshita, N. Kopidakis, and X. Hao, "Solar Cell Efficiency Tables (Version 58)," *Progress in Photovoltaics: Research and Applications* 29 (2021): 657–667.

45. F. Guo, S. Qiu, and J. Hu, et al., "A Generalized Crystallization Protocol for Scalable Deposition of High-Quality Perovskite Thin Films for Photovoltaic Applications," *Advanced Science* 6 (2019): 1901067.

46. C. Y. Chen, T. Y. Kuo, C. W. Huang, et al., "Thermal and Angular Dependence of Next-Generation Photovoltaics under Indoor Lighting," *Progress in Photovoltaics: Research and Applications* 28 (2020): 111–121.

47. B. Yang, J. Suo, F. Di Giacomo, et al., "Interfacial Passivation Engineering of Perovskite Solar Cells with Fill Factor over 82% and Outstanding Operational Stability on n-i-p Architecture," *ACS Energy Letters* 6 (2021): 3916–3923.

48. IEC, Photovoltaic Devices – Part 9: Classification of Solar Simulator Characteristics, IEC 60904-9:2020, (International Electrotechnical Commission, 2020).

49. IEC, Photovoltaic Devices – Part 3: Measurement Principles for Terrestrial Photovoltaic (PV) Solar Devices with Reference Spectral Irradiance Data, IEC 60904-3:2019, (International Electrotechnical Commission, 2019).

50. IEC, Photovoltaic Devices – Part 7: Computation of the Spectral Mismatch Correction for Measurements of Photovoltaic Devices, IEC 60904-7:2019, (International Electrotechnical Commission, 2019).

51. L. H. Slooff, J. M. Kroon, J. Loos, M. M. Koetse, and J. Sweelssen, "Influence of the Relative Humidity on the Performance of Polymer/TiO_2 Photovoltaic Cells," *Advanced Functional Materials* 15 (2005): 689–694.

52. P. Singh and N. M. Ravindra, "Temperature Dependence of Solar Cell Performance-An Analysis," *Solar Energy Materials and Solar Cells* 101 (2012): 36–45.

53. A. Usami, S. Seki, Y. Mita, H. Kobayashi, H. Miyashiro, and N. Terada, "Temperature Dependence of Open-Circuit Voltage in Dye-Sensitized Solar Cells," *Solar Energy Materials and Solar Cells* 93 (2009): 840–842.

54. E. A. Katz, D. Faiman, S. M. Tuladhar, et al., "Temperature Dependence for the Photovoltaic Device Parameters of Polymer-Fullerene Solar Cells under Operating Conditions," *Journal of Applied Physics* 90 (2001): 5343–5350.

55. I. Riedel, J. Parisi, V. Dyakonov, L. Lutsen, D. Vanderzande, and J. C. Hummelen, "Effect of Temperature and Illumination on the Electrical Characteristics of Polymer-Fullerene Bulk-Heterojunction Solar Cells," *Advanced Functional Materials* 14 (2004): 38–44.

56. C. Wehrenfennig, M. Liu, H. J. Snaith, M. B. Johnston, and L. M. Herz, "Charge Carrier Recombination Channels in the Low-Temperature Phase of Organic-Inorganic Lead Halide Perovskite Thin Films," *APL Materials* 2 (2014): 081513.

57. D. Bryant, S. Wheeler, B. C. O'Regan, et al., "Observable Hysteresis at Low Temperature in "Hysteresis Free" Organic-Inorganic Lead Halide Perovskite Solar Cells," *Journal of Physical Chemistry Letters* 6 (2015): 3190–3194.

58. L. Cojocaru, S. Uchida, Y. Sanehira, et al., "Temperature Effects on the Photovoltaic Performance of Planar Structure Perovskite Solar Cells," *Chemistry Letters* 44 (2015): 1557–1559.

59. L. K. Ono, S. R. Raga, S. Wang, Y. Kato, and Y. Qi, "Temperature-Dependent Hysteresis Effects in Perovskite-Based Solar Cells," *Journal of Materials Chemistry A* 3 (2015): 9074–9080.

60. H. Yu, H. Lu, F. Xie, S. Zhou, and N. Zhao, "Native Defect-Induced Hysteresis Behavior in Organolead Iodide Perovskite Solar Cells," *Advanced Functional Materials* 26 (2016): 1411–1419.

61. S. Shao, J. Liu, H. H. Fang, et al., "Efficient Perovskite Solar Cells over a Broad Temperature Window: The Role of the Charge Carrier Extraction," *Advanced Energy Materials* 7 (2017): 1701305.

62. L. Cojocaru, S. Uchida, K. Tamaki, et al., "Determination of Unique Power Conversion Efficiency of Solar Cell Showing Hysteresis in the I-V Curve under Various Light Intensities," *Scientific Reports* 7 (2017): 11790.

63. W. Shockley and H. J. Queisser, "Detailed Balance Limit of Efficiency of p-n Junction Solar Cells," *Journal of Applied Physics* 32 (1961): 510–519.

64. M. A. Green, "Accuracy of Analytical Expressions for Solar Cell Fill Factors," *Solar Cells* 7 (1982): 337–340.

65. J. F. Guillemoles, T. Kirchartz, D. Cahen, and U. Rau, "Guide for the Perplexed to the Shockley–Queisser Model for Solar Cells," *Nature Photonics* 13 (2019): 501–505.

66. S. Shao, M. Abdu-Aguye, Qiu Li, et al., "Elimination of the Light Soaking Effect and Performance Enhancement in Perovskite Solar Cells Using a Fullerene Derivative," *Energy & Environmental Science* 9 (2016): 2444–2452.

67. B. Roose, "Ion Migration Drives Self-Passivation in Perovskite Solar Cells and Is Enhanced by Light Soaking," *RSC Advances* 11 (2021): 12095–12101.

68. J. A. Kress, C. Quarti, Q. An, et al., "Persistent Ion Accumulation at Interfaces Improves the Performance of Perovskite Solar Cells," *ACS Energy Letters* 7 (2022): 3302–3310.

69. C. Xiao, Y. Zhai, Z. Song, et al., "Operando Characterizations of Light-Induced Junction Evolution in Perovskite Solar Cells," *ACS Applied Materials & Interfaces* 15 (2023): 20909–20916.

Supporting Information

Additional supporting information can be found online in the Supporting Information section. **Supporting Fig. S1:** J–V curves of the six samples (a) OPV-1, (b) OPV-2, (c) PSC-1, (d) PSC-2, (e) RC-1, and (f) RC-2 measured by the 20 laboratories (the PVEVL and Lab-A ~ Lab S) under the standard test conditions (STC). **Supporting Fig. S2:** Correlation diagrams of (a,b) Jsc, (c,d) Voc, and (e,f) FF deviations between emerging PV samples and RC-1 (c-Si + KG) and RC-2 (GaAs). **Supporting Fig. S3:** Normalized EQE spectra of the six samples (a) OPV-1, (b) OPV-2, (c) PSC-1, (d) PSC-2, (e) RC-1, and (f) RC-2 measured by the PVEVL and other participants. **Supporting Fig. S4:** Photos of (a) the OPV/PSC sample fixed on a temperature programmable stage with the four-wire connection for J-V measurements and a T-type thermocouple inserted between the sample and a thermal pad for monitoring and controlling the temperature of the sample, and (b) a lightshielding cover placed at the top to eliminate undesired light reflection in J-V measurements. **Supporting Table S1:** Initial, midterm, and final photovoltaic parameters and the expanded measurement uncertainty (coverage factor (k) of 2 for an approximate 95% confidence level) of the samples obtained by the PVEVL.